

# Wine glass sound excitation by mechanical coupling to plucked strings

Lior Arbel<sup>1</sup>, Yoav Y. Schechner<sup>2</sup>, and Noam Amir<sup>3</sup>

<sup>1</sup>Faculty of Architecture and Town Planning,  
Technion - Israel Institute of Technology, Haifa, Israel

<sup>2</sup>Viterbi Faculty of Electrical Engineering,  
Technion - Israel Institute of Technology, Haifa, Israel

<sup>3</sup>Department of Communication Disorders,  
Sackler Faculty of Medicine, Tel-Aviv University, Tel-Aviv, Israel

## Abstract

Wine glasses can be used to produce musical sounds using various excitation mechanisms. In this work a method for producing wine glass sounds is proposed, consisting of coupling a string to a wine glass. The coupled string-glass system produces sounds by transmitting vibrations from the string to the glass. The glass reacts sympathetically, much like sympathetic strings on instruments like the Sitar. Two methods for creating acoustic coupling between the string and glass are developed; one by direct contact between the two and one by using a custom designed coupling component. In the latter, a coupling mechanism transmits vibrations from the string to the glass while maintaining some geometric distance between the two. The coupling component is designed through an optimization process composed of two stages in order to maximize the intensity of the glass sound. The proposed coupling method can be used as the basis for designs of wine glass instruments, adding to the existing excitation methods of striking, bowing and rubbing. Some prototypes of such instruments are suggested here. These instruments may have the combined spectra and sound characteristics of both strings and wine glasses, offering timbres and playing techniques different from those of existing wine glass instruments.

# 1 Introduction

Wine glasses have been used for centuries as components of musical instruments. According to an historical review given by Gallo and Finger[1], the origins of wine glass instruments trace back to ancient Persia and China, with the first reference to a European glass instrument, the Verrillon, appearing in *Theorica Musice* (1492) by Franchino Gaffurio. The Verrillon, a set of ordinary glasses mounted on a table and tuned with water, was played by striking with a mallet. A more modern version, the Glass Harp, first appeared during the 18<sup>th</sup> century. It differs from the Verrillon by the particular use of wine glasses and by the playing method, which consists of rubbing a moistened finger around the rim of the glass, instead of striking. A similar noteworthy instrument is the Glass Harmonica, invented by Benjamin Franklin in 1761. It consists of a set of glass bowls mounted on a rotating spindle and played by placing a moistened finger over the rim of the rotating bowls.[2] Several papers on the acoustics of wine glasses investigate both empty and liquid-filled vessels.[3, 4, 5] The common principle of all existing wine glass instruments is the sound production method: either by rubbing with a moistened finger, striking or bowing.[6] This paper presents and develops a new method for producing wine glass sounds, by coupling the wine glass to a vibrating string.

Development of string-glass coupling is inspired by sympathetic strings that exist in various musical instruments. In these, two coupled sets of strings are mounted on a single instrument. One set of strings ("the playing strings") is directly excited by the player. Vibrations are then transmitted to a second set of strings ("the sympathetic strings") which react and produce a sound.[7, 8] Some notable examples are Hindustani classical instruments such as the Sitar, Sarod and Sarangi. The sound generated by the sympathetic strings is considered to be an important feature of the instrument. Weisser and Demoucron[9] quote various researchers describing the sympathetic strings of Hindustani instruments and their sound as wonderfully complex, lingering halo of sound and a basic phenomenon of Indian music.

In addition to string-to-string coupling, in some cases sympathetic strings

are excited by non-string components. One such example is 'Prongs & Echoes', an instrument by designer Bart Hopkin,[10] where sympathetic strings are excited by small metal prongs. While many examples exist for instruments in which *strings* are sympathetically excited, only a few examples exist where non-string components are sympathetically excited (by strings or by any other components). One such example is a xylophone, where the bars are sympathetically coupled to the tube resonators.[11, 12] In the present study we propose a new musical component to be excited sympathetically: Wine glasses. While the acoustic characteristics of commercially available wine glasses vary greatly, some have narrow resonances with high Q factors.[13, 14] This permits the glasses to store energy transferred to them from an external vibration source. Due to the high Q factor, the glasses can continue to radiate sounds after the source's vibration has stopped. Thus, the proposed instruments described in this study use wine glasses in a similar manner to which the above-mentioned Hindustani instruments use sympathetic strings - in order to create special acoustic effects. In addition, the wine glasses can also be used for sound radiation, as their large surface area makes them better radiators than strings. Thus, in the case where the proposed instrument is not fitted with an additional soundboard, the wine glasses will fill a double role both as sympathetic resonators and as the principal radiators.

In the next sections we describe the principles and development of several string-glass coupling mechanisms. We begin in section 2 by presenting two basic designs of instruments: one with direct string-glass excitation, and the second with an intermediate coupling component. Section 3 describes the operating principles of both coupling methods. Sections 4 and 5 describe the development of the coupling component using optimization algorithms. Section 6 describes an experiment for evaluating the performance of the different mechanisms. Section 7 is devoted to a discussion of the results.

## 2 String and wine glass instrument concepts

Two instrument concepts are suggested here in order to demonstrate the potential of string to wine glass coupling. The first, illustrated in Figure 1,

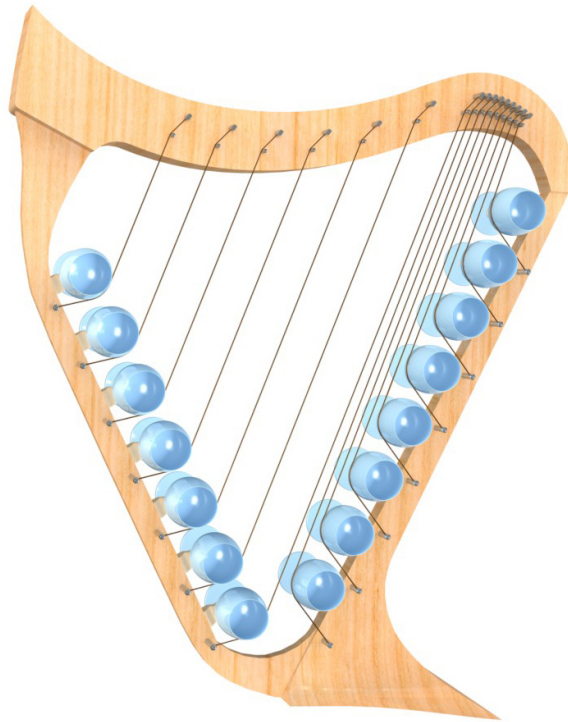


Figure 1: A concept of a string-wine glass instrument, using direct coupling.

is based on the shape of a harp. The string-glass coupling is achieved by direct contact. This approach is explored in section 3.1. The figure shows an instrument with 15 strings, each coupled to a different wine glass. The wine glasses are placed on both sides of the frame, replacing the sound box and pillar in a typical harp. The second concept, illustrated in Figure 2, couples the strings to the glasses using a coupling component. The figure shows an instrument composed of 7 coupling components positioned on top of a sound box and 7 wine glasses positioned adjacently. Each coupling component couples one or more strings to a single glass. The existence of the sound box is made possible due to the distance between string and glass permitted by the coupling component. This coupling mechanism is studied in sections 3.2, 4 and 5.

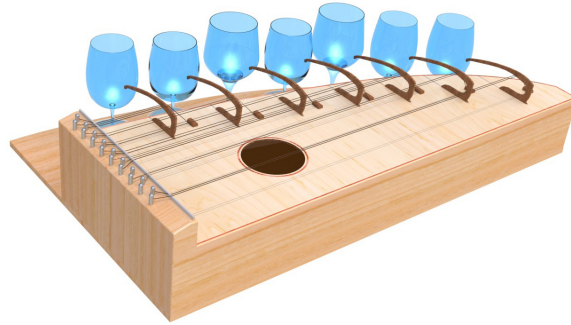


Figure 2: A concept of a string-wine glass instrument, using an optimized coupling component.

### 3 String-glass coupling mechanisms

#### 3.1 Direct contact coupling

Consider a tight string directly touching the surface of a household wine glass, as shown in Figure 3. The string is fastened to a frame equipped with a tail-piece and a nut. The glass, free to vibrate, touches the string near the string's end and exerts an upwards force on the string. The glass thus performs a similar role to that of a bridge on a string instrument. The string is free to vibrate in the section between the nut and the glass' contact point. In initial tests we found that the preferred contact point is at the widest part of the glass. Measurements of the produced sounds are described in section 6.

Direct contact coupling is a feasible basis for design of such musical instruments, however it requires direct contact between the string and the wine glass. This may limit design options, which prompts the need for a coupling method that allows a physical distance between the two components.

#### 3.2 Coupling component and need for optimization

In order to create a certain physical distance between the strings and the wine glasses, a coupling component ('bridge') is used to mount the string and to transmit the vibrations to the glass through a contact point. A generic bridge coupling a string to a wine glass is shown in Figure 4. Clearly, the magnitude of the mechanical impedance of the bridge has an effect on

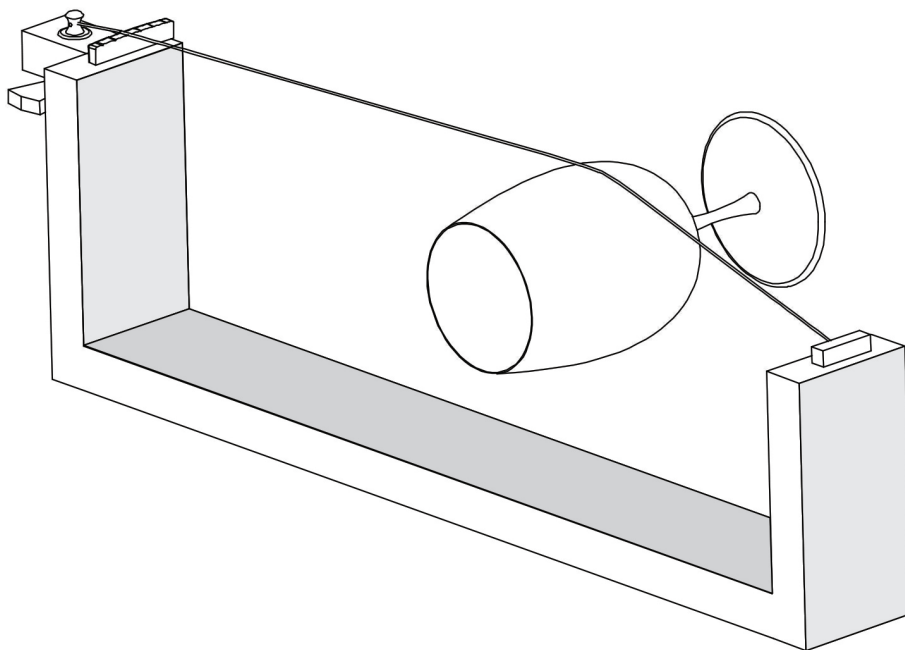


Figure 3: The string and wine glass coupled by direct contact, mounted on a frame.

The glass is held using a custom-made clamp (not shown).

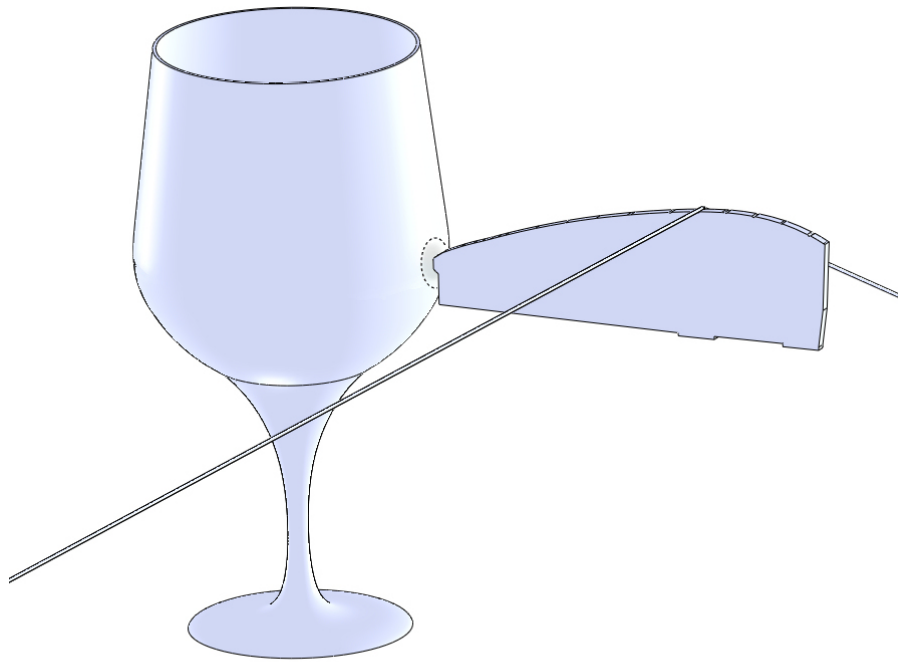


Figure 4: A generic bridge, coupling a string to a wine glass.  
The bridge-glass contact point is highlighted.

the produced glass sounds. This impedance is adjustable by introducing geometric changes to the bridge. Simulations verify that when the bridge impedance is lowered to the order of magnitude of the glass impedance, the sound intensities produced by the glass increase. Figure 5 shows the simulated glass transfer impedance along with the transfer impedance of a manually designed bridge prototype, used in early stages of this research. Note that the bridge impedance is considerably higher.

If the bridge design is not performed properly, sounds produced using the bridge may be weaker than those produced by direct coupling, as indeed was shown in preliminary simulations and experiments. This prompts the need for a quantitative design process, which can optimize the performance of the coupling component.

In the following two sections we explore the design of a coupling component using a two-stage optimization process. First, an initial prototype is

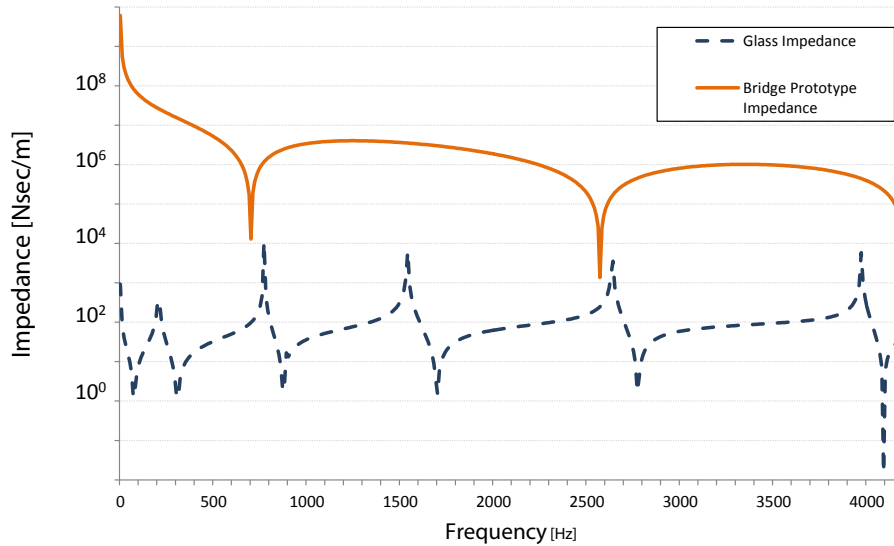


Figure 5: The transfer impedances (magnitude) of the glass and bridge prototype.

developed using the *material distribution method*. Then, this prototype is refined using the *shape optimization method*. In order not to limit the design possibilities of future instruments, the process presented here assumes a general case where a single glass is expected to generate responses over a large range of excitation frequencies. It is envisioned that for specific future designs, in cases where the glasses will be expected to respond only to specific notes or frequencies, the optimization process will be repeated with suitable criteria.

## 4 Optimization of the material distribution

A thorough description of the *material distribution method* is given by Bendsoe and Sigmund.[15] When applying this method, the structure is optimized to minimize or maximize a desired physical quantity. This method is suitable for the optimization of musical instruments and components, such as the optimization of a violin bridge to a desired frequency response.[16] Optimization begins by setting the external boundaries of the structure. The design variable is the material density distribution (or elasticity function)

over the entire shape. For every point in space, the optimization process determines if there should be material at that point or not. The resulting design consists of a new spatial distribution of matter within the boundaries: points that are filled with material and points that remain void (containing no material).

The *material distribution method*[17] has an advantage that it can generate a completely new shape of coupling component. We now describe how the *material distribution method* can optimize coupling to maximize wine glass sound intensities.

#### 4.1 Optimization setup

When applying the optimization process to the coupling component, we started with the constraint that the desired output be a flat shape, having a fixed cross section. Such shapes can be easily fabricated from wood. Therefore, optimization was run over the domain of two dimensional shapes. The coupling component can be efficiently modeled and optimized for a flat shape since the relevant string forces exerted on the component are transverse. Longitudinal string vibrations in typical string instrument sizes are of a lesser musical importance.[7, 10] The optimization setup includes a manually designed initial shape and designated glass and string contact points, as shown in Figure 6. Note that with any coupling method, the coupling strength may differ between horizontal and vertical string movements. For different instruments, the string movement is determined by the playing technique,[18] which in turn may also be affected by the design of the instrument itself. In order to ensure greater compatibility with possible future designs, string excitation was modeled as an in-plane sinusoidal load with equal horizontal and vertical components. The material properties used were of Ipe wood[19] (to be later used for actual fabrication), with the grain aligned in the direction of the horizontal axis. The *material distribution method* optimization process is computationally intensive, with execution times as high as 20-30 minutes per frequency. Moreover, several iterations were required to fine tune various implementation-specific parameters before a successful execution was performed. Therefore, the frequency range

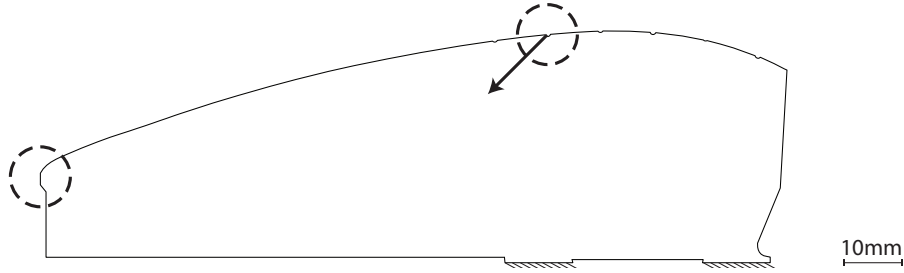


Figure 6: The boundaries of the initial shape for the material distribution optimization process, showing zero-displacement segments (bottom), string excitation point and direction (top, circled) and glass contact point (left, circled).

was set to 100 - 1000Hz with a 100Hz resolution, as a feasible compromise between resolution and execution time. Additional sporadic tests performed with intermediate frequencies generated similar layouts, suggesting that using a higher resolution may only provide a minor contribution to the end result. The chosen range covers fundamental frequencies of all notes between G#<sub>2</sub> (103.83Hz) to B<sub>5</sub> (987.7Hz).

The *material distribution method* generates a new structure by way of creating a spatial elasticity function (Young's modulus) covering the entire domain,  $\Omega$ . The new structure created within the boundaries of  $\Omega$  is represented by points containing material having its nominal elasticity. Points excluded from the structure (void) are represented as being composed of zero elasticity material. The *material distribution method* can also yield models containing points of intermediate elasticity values. However, intermediate elasticity values are difficult to manufacture by traditional methods. Thus, an approach was needed which would discourage the optimization process from seeking such intermediate values. Such an approach is the Solid Isotropic Material with Penalization (SIMP).[20] The design variable is  $\alpha(x, y)$ , with values of [0-1] over the entire domain,  $\Omega$ . The material's Young's modulus is represented as  $E = \alpha(x, y)^p E_0$ . Here  $E_0$  is the material's nominal Young's modulus and  $p = 5$  is the SIMP penalization parameter. The design variable  $\alpha(x, y)$  therefore affects Young's modulus, thus also affecting the structure's mechanical properties. In addition, a constraint on

the design variable is defined as

$$\text{CSTR} = \iint_{\Omega} \alpha(x, y) d\Omega; \quad x, y \in \Omega \quad (1)$$

An upper limit was imposed:

$$\text{CSTR} \leq \text{CSTR}_{\text{limit}} = 0.5 \iint_{\Omega} d\Omega; \quad x, y \in \Omega \quad (2)$$

Note that CSTR is linear in  $\alpha(x, y)$  while Young's modulus,  $E$ , is proportional to  $\alpha(x, y)^p$ . At each point,  $\alpha(x, y)$  contributes to both CSTR and  $E$ . However, since  $p > 1$ , points where  $0 < \alpha(x, y) < 1$  contribute a disproportionately lower change to  $E$  than to CSTR.[21] As CSTR is limited by  $\text{CSTR}_{\text{limit}}$ , the algorithm is encouraged to avoid points of ineffective intermediate  $\alpha(x, y)$  values, which inflate CSTR but contribute little to  $E$ . Rather, the algorithm favors points where  $\alpha(x, y) = 1$ , representing the shape of the optimized structure, or  $\alpha(x, y) = 0$ , representing void. Various  $\text{CSTR}_{\text{limit}}$  values were shown to generate layouts with minor differences. Values of  $\text{CSTR}_{\text{limit}}$  between  $0.3 \iint_{\Omega} d\Omega$  to  $0.8 \iint_{\Omega} d\Omega$  generated layouts with even smaller differences. As the layout generated by this stage is later refined and further optimized, these differences have little effect on the optimization end result. The value for  $\text{CSTR}_{\text{limit}}$  was therefore set to  $0.5 \iint_{\Omega} d\Omega$ , in the middle of the above-mentioned range.

## 4.2 Objective function

The current optimization stage was performed in a two-dimensional space. A wine glass cannot be fully modeled as a two dimensional object.[5] Therefore, a wine glass model cannot be included in the optimization space without losing the wine glass acoustic properties. Thus, the optimization model consisted solely of the bridge. It was then necessary to choose an objective function that is based only on the bridge, and not on the glass. Based on simulations described in section 3, an objective function was chosen with the aim of matching the magnitude of the bridge impedance (which is mostly purely imaginary with  $-\frac{\Pi}{2}$  phase) to the average magnitude of the glass impedance (which is mostly purely imaginary with  $+\frac{\Pi}{2}$  phase). The glass is therefore accounted for in the optimization via its impedance. Let  $b \in B$

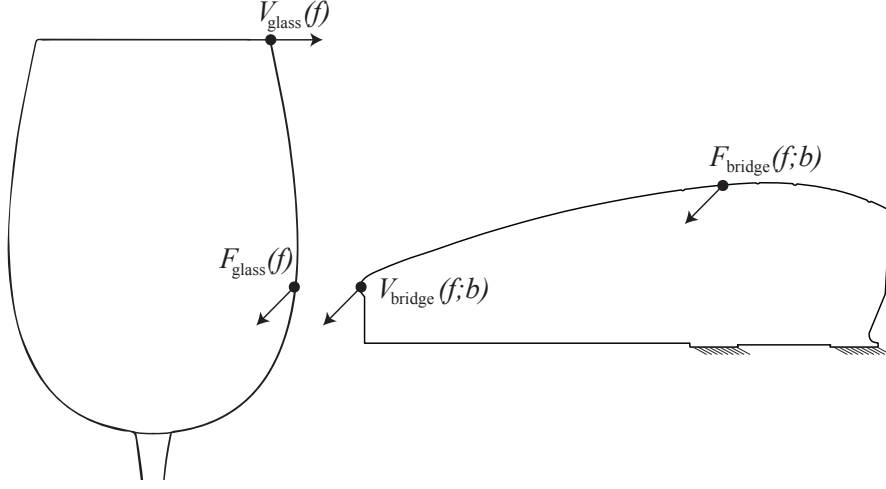


Figure 7: The force and velocity vectors defining the transfer impedances, shown on both the glass and the bridge (initial shape).

denote a bridge layout, where  $B$  is the set of all possible layouts. Let  $f$  denote the string excitation frequency. The glass transfer impedance is defined by a force  $F_{\text{glass}}(f; b)$  measured on the bridge contact point divided by the velocity  $V_{\text{glass}}(f; b)$  measured on a single point on the rim. The average glass transfer impedance over the frequency range is  $\bar{Z}_{\text{glass}}$ . The bridge frequency-dependent transfer impedance is  $Z_{\text{bridge}}(f; b)$ , defined by a force  $F_{\text{bridge}}$  measured on the string excitation point divided by the velocity  $V_{\text{bridge}}$  measured on the glass contact point. Figure 7 shows the applied forces and induced velocities defining both impedances.

The difference in magnitudes is given by

$$Z(f; b)_{\text{diff}} = |Z_{\text{bridge}}(f; b)| - |\bar{Z}_{\text{glass}}| \quad (3)$$

Averaging the magnitude difference over a set  $F$  of discrete frequencies,  $F = \{100, 200 \dots 1000\}$ :

$$\bar{Z}_{\text{diff}}(b) = \frac{1}{|F|} \sum_{f \in F} Z_{\text{diff}}(f; b) \quad (4)$$

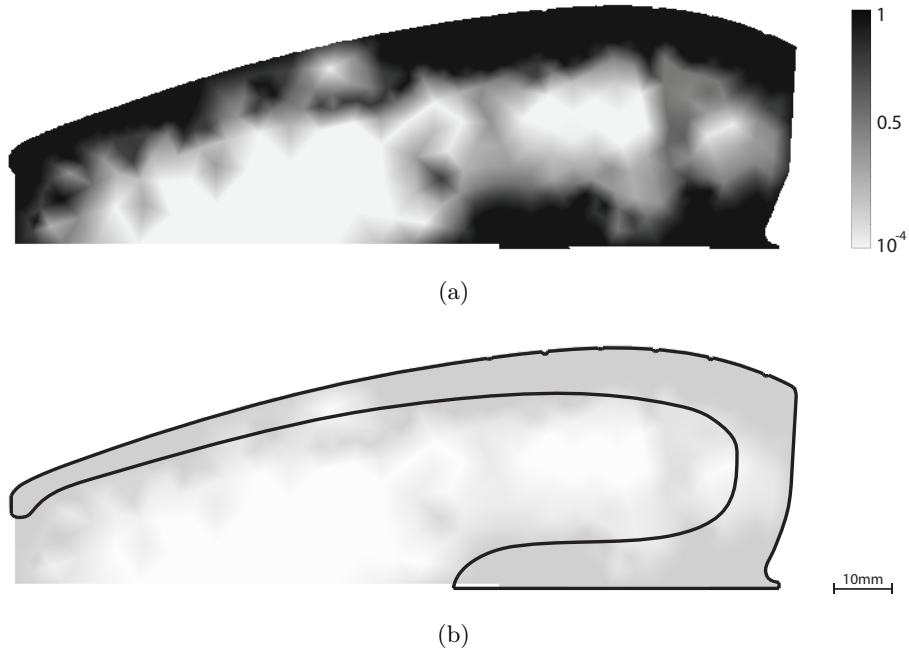


Figure 8: (a) The Young's modulus coefficient function  $\alpha(x, y)$  derived by optimization. High elasticity regions are shown in dark shades. (b) The O1 prototype extracted from  $\alpha(x, y)$  by outlining the high density areas and smoothing the edges.

The optimization goal is defined as finding  $\hat{b}$  that minimizes  $\bar{Z}_{\text{diff}}(b)$ :

$$\hat{b} = \arg \min_{b \in B} \bar{Z}_{\text{diff}}(b) \quad (5)$$

### 4.3 Optimization results

Equation (5) resulted in a two dimensional layout for a new prototype of an optimized coupling component, as shown in Figure 8a. A refined shape labeled 'O1' is shown in Figure 8b. Shape O1 is extracted by thresholding  $\hat{b}$  at 0.95 and smoothing the edges, retaining full elasticity points representing the optimized shape and omitting the zero elasticity points representing the void. The O1 prototype served to initialize a second optimization stage, aimed at determining a final shape, as discussed next.

## 5 Shape optimization

The *shape optimization method* is the algorithm used in the second optimization stage and is described in detail by Bendsøe and Sigmund.[15] Shape optimization seeks the optimal shape parameters for the purpose of minimizing or maximizing a desired physical quantity. However, unlike the *material distribution method*, shape optimization is applied to a shape that already exists yet needs tuning. Several geometric features are defined as having parametric magnitudes (length, angle, thickness etc.) and serve as the design variables. The optimization algorithm then finds the optimized set of values for these parameters, given a search domain. This method was used for optimizing the frequency responses of metallophones and cubic filters.[22, 23]

### 5.1 Optimization setup

The model, illustrated in Figure 9, includes the coupling component and a wine glass. The wine glass is based on actual dimensions of household wine glasses, to be used later in the physical implementation. An initial prototype such as the one created by the *material distribution method* (O1) is used as the coupling component. The initial coupling component O1 is extended to a third dimension by extrusion, with a fixed thickness of 3mm. Afterwards, the optimization was performed over a domain of 2D shapes extruded to this fixed thickness. As in this configuration the *shape optimization method's* execution times are about half than those of the *material distribution method*, a higher resolution of 50Hz was chosen, with an identical 100-1000Hz frequency range. As with the *material distribution method*, additional sporadic tests using intermediate frequencies generated similar end results and offered little contribution to the final shape. The bridge material properties, wood alignment and string excitation model are as described in section 5.1.

Mathematically, the shape is parameterized as follows: The outer contour,  $\tilde{\mathbf{O}}$ , is embedded with  $N$  fixed anchor points  $x_i^{\text{anchor}}$ , as shown in Figure 10. From each anchor point, a ray  $R_i$  is projected at a fixed direction towards the inner contour of the coupling component,  $\tilde{\mathbf{I}}$ . The intersection of  $R_i$  and  $\tilde{\mathbf{I}}$  results in  $N$  intersection points,  $x_i^{\text{int}} = R_i \cap \tilde{\mathbf{I}}$ . The distances,

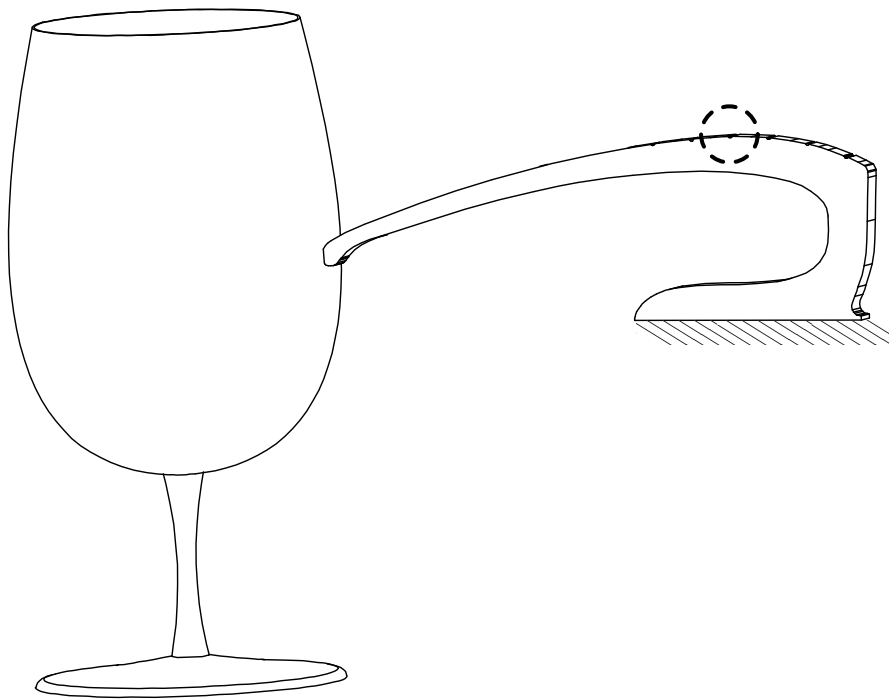


Figure 9: The model used in the shape optimization method stage, consisting of the coupling component O1 and a wine glass. The string excitation point is circled.

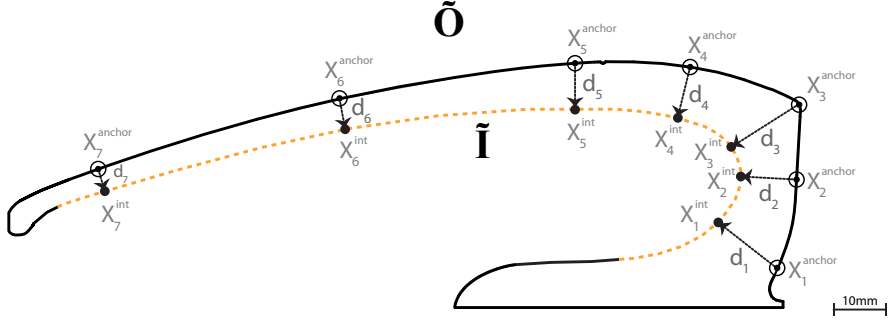


Figure 10: The O1 coupling component with segments  $d_1 \dots d_7$  connecting between the fixed outer contour  $\tilde{\mathbf{O}}$  (solid line) to the adjustable inner contour  $\tilde{\mathbf{I}}$  (dashed line).

$d_i = |x_i^{\text{anchor}} - x_i^{\text{int}}|$  are the design variables. The algorithm changes the distances, thus changing the position of each  $x_i^{\text{int}}$  along  $R_i$ . Once the positions of  $x_i^{\text{int}}$  are changed, the inner contour  $\tilde{\mathbf{I}}$  is replaced by a spline connecting all intersection points at their new positions. As a result, the shape of the bridge is tuned.

## 5.2 Objective function

The objective to be optimized is taken to be maximum glass displacements, because larger displacements produce higher sound intensities. All wine glass modes are characterized by having anti-nodes on the rim, with some higher modes characterized by additional anti-nodes on the surface, as demonstrated in Figure 11. Therefore, we measure displacement using a closed line integral over the rim, necessarily covering anti-node displacements contributed by all modes.[24] Let  $\beta$  be a shape of a bridge defined by a set  $\{d_1 \dots d_N\}$ . Let  $\mathcal{B}$  be the domain of all possible bridge shapes that can evolve from O1 by small perturbations. These perturbations are bounded. Let  $f$  be the excitation frequency and  $\theta$  be the angular coordinate (azimuth) of a point on the glass rim. The frequency-dependent glass displacement at a point on the rim of the glass is  $D_{\text{point}}(f, \theta; \beta)$ , as shown in Figure 12.

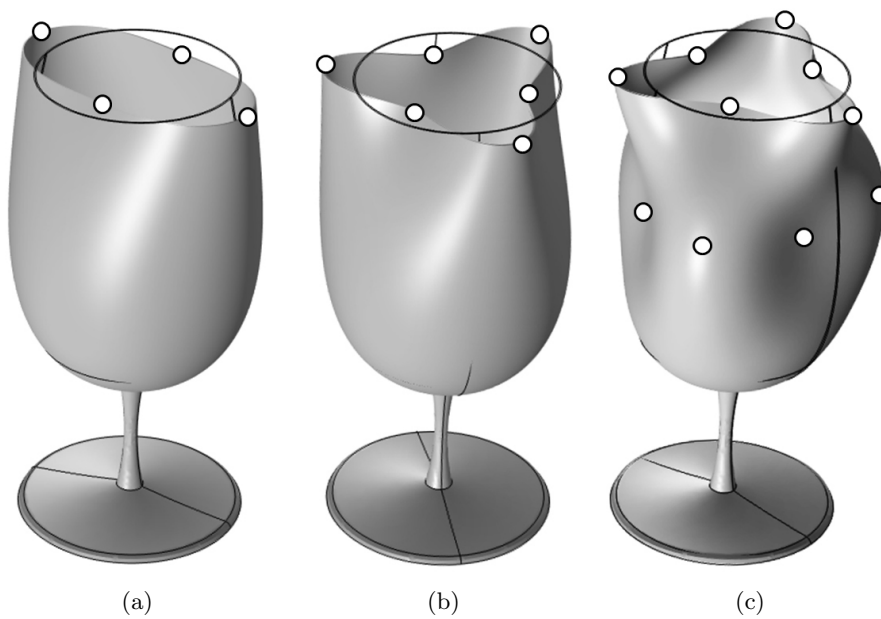


Figure 11: Several normal modes of a wine glass, with anti-nodes marked by white circles. The rim shape at rest is marked by a black contour. (a) Mode  $(2,0)$ , with 4 anti-nodes on the rim. (b) Mode  $(3,0)$ , with 6 anti-nodes on the rim. (c) Mode  $(3,1)$ , with 6 anti-nodes on the rim and 6 anti-nodes on the surface.

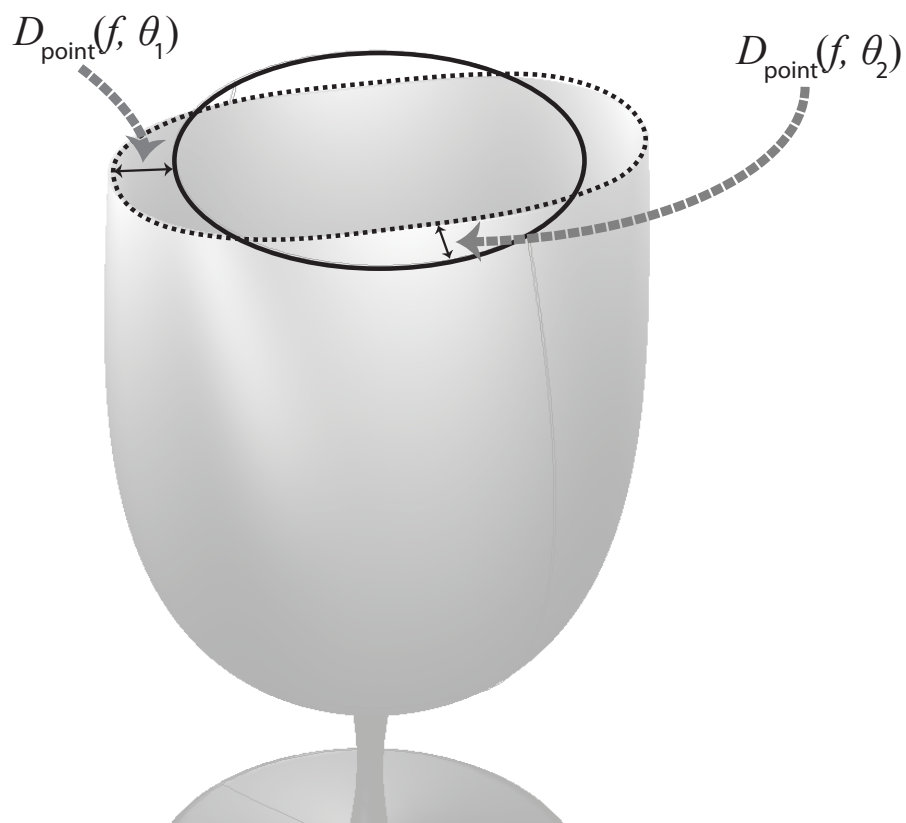


Figure 12: A glass deformed due to excitation (exaggerated).  
The circle in black shows the shape of the rim at rest.

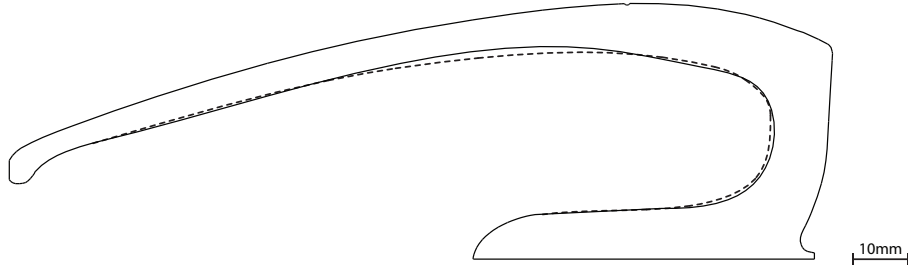


Figure 13: The final optimized bridge (solid line) on top of O1 (dashed line).

Defining the closed line integral

$$D_{\text{rim}}(f; \beta) = \oint_0^{2\pi} |D_{\text{point}}(f, \theta; \beta) d\theta| \quad (6)$$

Let us average  $D_{\text{rim}}(f)$  over a set of discrete frequencies,  $F_2 = \{100, 150 \dots 1000\}$  Hz:

$$\bar{D}(\beta) = \frac{1}{|F_2|} \sum_{f \in F_2} D_{\text{rim}}(f; \beta) \quad (7)$$

The optimization seeks a set  $\beta = \{d_1 \dots d_N\}$  which defines a new bridge  $\hat{\beta}$  that maximizes  $\bar{D}(\beta)$ :

$$\hat{\beta} = \arg \max_{\beta \in \mathcal{B}} \bar{D}(\beta) \quad (8)$$

### 5.3 Optimization results

The second optimization stage used  $N=7$  anchor points and the material properties of Ipe wood. It resulted in a new set of values for the section lengths, defining a new spline and a new optimized bridge, as shown in Figure 13. The length of most rays was reduced, in some cases by as much as 20%. The newly created bridge, which was the final product of the optimization process, was labeled the *optimized bridge*.

The optimized bridge was tested by simulation and compared to the Direct Contact coupling method. Each mechanism was simulated separately using the same wine glass model and a frequency sweep over 20-3000Hz, covering all notes in the range up to F#<sub>7</sub> (2959.96Hz). Figure 14 shows the normalized simulated displacements of the glass rim produced by each coupling mechanism. The average simulated glass rim displacements over

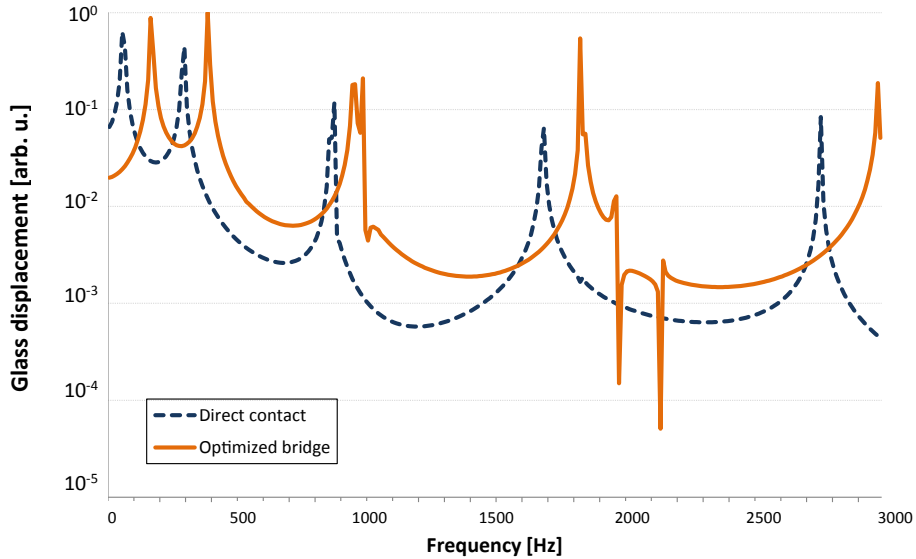


Figure 14: Simulation results showing glass displacements at the rim, generated by each coupling mechanism.

the simulated frequency range generated by the optimized bridge are about 75% larger than the displacements generated by direct contact. Experimental results for the same comparison are described in section 6. Note that the curves have a similar overall shape, with the resonance frequencies of the optimized bridge-glass system occurring at higher frequencies. The shift of the first resonance frequency is about 100Hz, with the shift progressively increasing for each subsequent resonance frequency. The 3<sup>rd</sup> resonance frequency of the optimized bridge-glass system is split into two frequencies, forming a doublet.

## 6 Experiments

To complement the findings of the simulations, an experiment was conducted using the setup shown in Figure 15. The experiment compared wine glass sound intensities produced using the two different coupling mechanisms.

A custom built experimental rig held the glass and string in place. Each mechanism was tested with three household mass-produced wine glasses, shown in Figure 16. The glasses were used without tuning or alteration.

Two of the glasses (labeled Glass1a, Glass1b) were of the same make and model and seemingly identical. These glasses had different lowest resonance frequencies, (438Hz and 547Hz respectively), due to minute differences in thickness or material properties. The geometry of these glasses was used as a model during the optimization process. The third glass (labeled Glass2) was of a different model with a different geometry - shorter and wider. Glass2 had the lowest resonance frequency at 434Hz. Steel strings of various gauges were used, tuned to frequencies of musical notes in the range of A<sub>1</sub> (55Hz) to E<sub>5</sub> (659.25Hz). The string and wine glass were coupled by each of the mechanisms. Each measurement consisted of plucking the string and then quickly muting it. The string sound and glass response were recorded using a microphone placed 5cm above the glass rim. While various papers describe the development of mechanical plucking systems,[25, 26] we are unaware of standard devices available as commercial products. We therefore chose to pluck and mute the string manually. As the manual plucking force is not perfectly repeatable, 3 repetitions were performed per note. The recordings were normalized by the maximum amplitude of the string sound, thus rendering the glass response intensities comparable. Each note's glass response sound intensity was calculated by averaging the RMS value over a 40ms window immediately after the string muting, across the 3 repetitions. For each glass, some notes within the range did not produce measurable glass sounds above the background noise level with either coupling method; the total number of notes with sufficient intensity above the background noise level, per glass was 25 (Glass1a), 12 (Glass1b) and 21 (Glass2), respectively. Figure 17 shows the intensities measured for Glass1a using both coupling mechanisms.

The normalized average sound intensity was calculated for each glass and excitation method as follows: for each glass, let  $I_t$  be the intensity of the sound produced by excitation at note t. Let  $M$  be the set of all notes that produced intensities above the background noise, per glass. Let  $OB$  and  $DC$  be the optimized bridge and direct contact excitation methods, respectively. The maximal sound intensity measured per glass is defined as:

$$I_{\max} = \max \{ \{I_t\}_{t \in M} \}_{OB,DC} \quad (9)$$

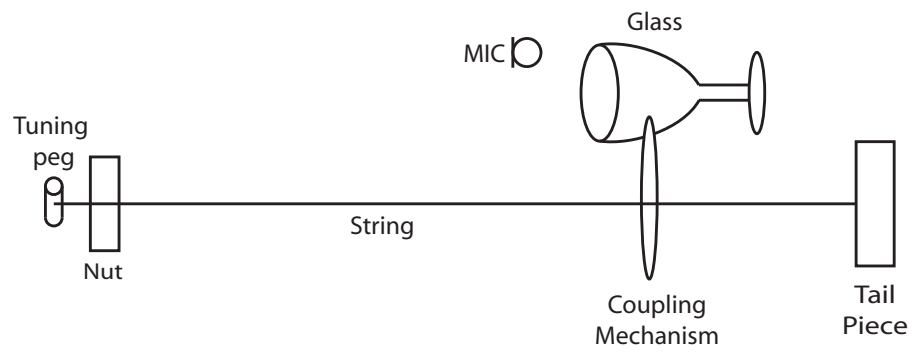


Figure 15: Experimental setup showing the coupled string and wine glass.



Figure 16: The three glasses used in the experiment: Glass1a (left), Glass1b (middle) and Glass2 (right).

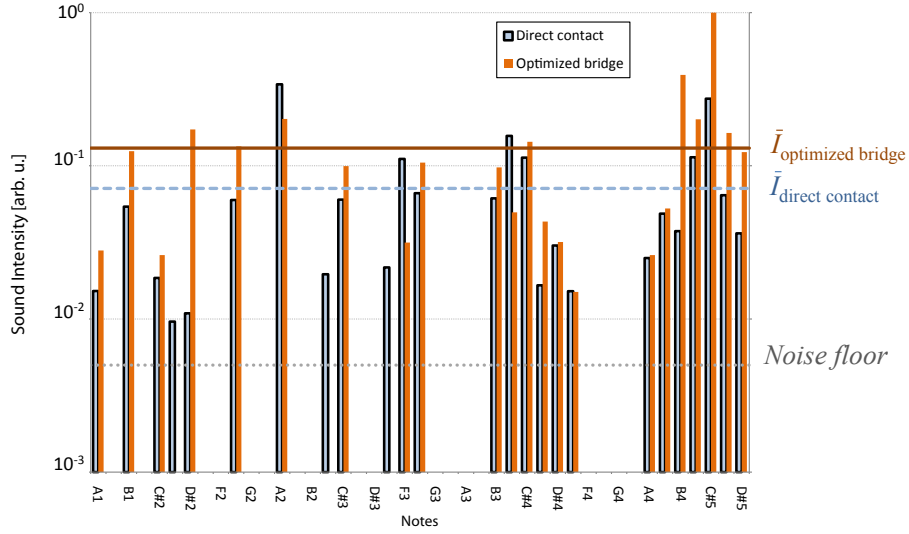


Figure 17: Intensity measurement results for Glass1a.

Table 1: Results of measured wine glass sound intensities

Glass	Optimized bridge	Direct contact
<b>Glass1a</b>	$\bar{I}=0.13$	$\bar{I}=0.07$
	$I_{med}=0.09$	$I_{med}=0.05$
<b>Glass1b</b>	$\bar{I}=0.21$	$\bar{I}=0.14$
	$I_{med}=0.12$	$I_{med}=0.1$
<b>Glass2</b>	$\bar{I}=0.25$	$\bar{I}=0.35$
	$I_{med}=0.24$	$I_{med}=0.3$

The normalized average sound intensity per glass, per excitation method, is defined as:

$$\bar{I} = \frac{1}{|M| I_{\max}} \sum_t I_t \quad t \in M \quad (10)$$

In addition, the median  $I_{med}$  of the normalized sound intensities was calculated for each glass and excitation method. The results are shown in Table 1.

The results for Glass1a and Glass1b showed similar trends, with the optimized bridge generating the highest average and median glass sound responses. Glass2, which is different in geometry from the model used in

the optimization process, showed the opposite trend.

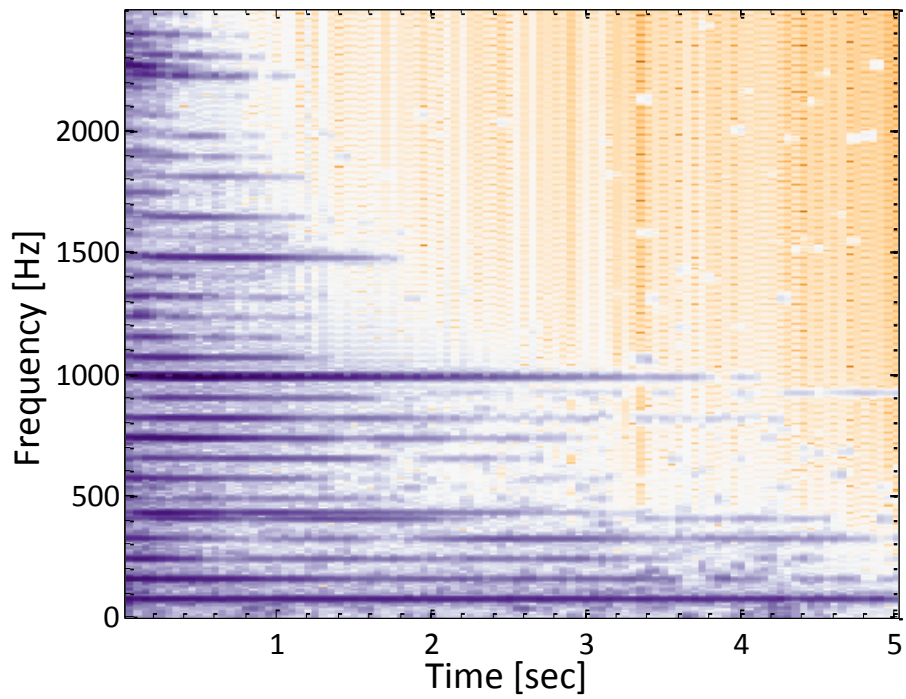
For all glasses, the loudest intensities were produced when the string's fundamental frequency or one of its overtones closely coincided with the glass resonance frequency of mode (2,0). This mode is characterized by having 4 anti-nodes on the rim, as shown in Figure 11a. The resonance frequency of mode (2,0) is most usually the strongest resonance frequency in a wine glass spectrum. For example, the (2,0) mode resonance frequency of Glass1a is 547Hz. String excitation at C#<sub>5</sub> (554.4Hz) maximized the sound intensity produced by this glass relative to all other excitation frequencies. In addition, exceptionally high responses were produced by excitation tones which coincided with glass resonance frequencies of higher normal modes.

A spectrogram of the combined sound of a string and a wine glass (Glass2) coupled by direct contact is shown in Figure 18a. The string is tuned to E<sub>2</sub> (82.41Hz). A spectrogram of a classic guitar playing E<sub>2</sub> is shown in Figure 18b for comparison. The partials contributed by the wine glass are especially visible at 434Hz, 990Hz and 2267Hz. The glass was separately shown to have partials at these frequencies. Note that some glass partials closely coincide with string harmonics. For instance, the strong glass doublet at 990Hz and 998Hz coincides with the string's 12<sup>th</sup> harmonic at 984Hz, as is clearly visible in the spectrogram. The actual sound recordings are found in the attached sound clips: 'Sound clip1 - String and wine glass.wav' and 'Sound clip2 - Guitar string reference.wav'.

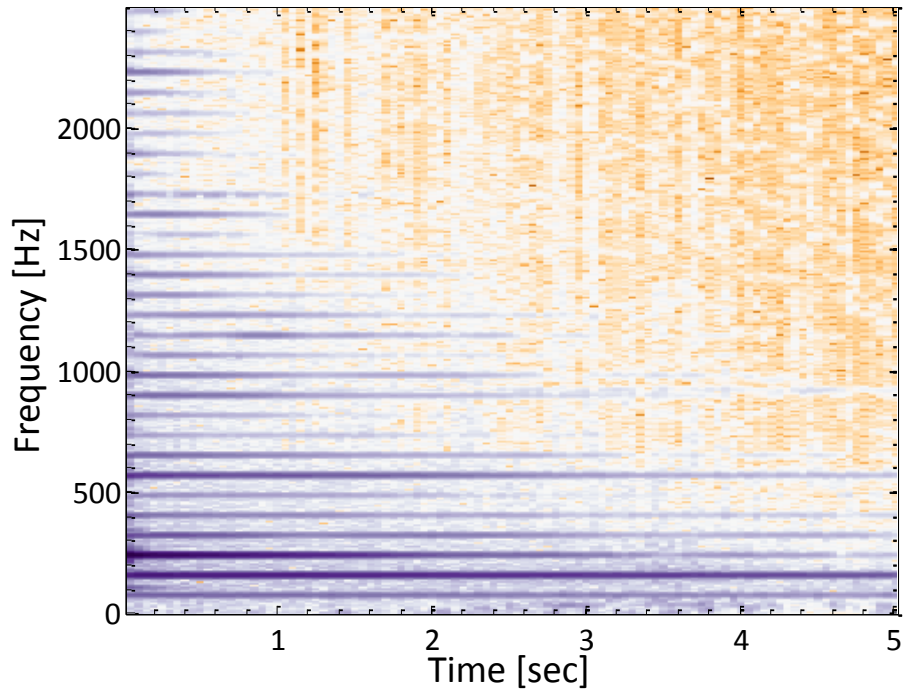
## 7 Discussion

The above data shows that the optimized bridge does indeed produce higher sound intensities than the direct contact method when used with glasses that have an identical geometry to the model used in the optimization process. However, with a considerably different glass such as Glass2, the optimized bridge does not offer an improvement, in terms of sound intensity, over the direct contact method.

Future research could involve extending the methods described in this paper by generalizing the optimization stage to include glasses of a larger variety (different geometries, sizes and materials). Additional experiments



(a)



(b)

Figure 18: (a) Spectrogram of the combined sound of wine Glass2, excited by a string tuned to  $E_2$ . (b) Spectrogram of a classic guitar E string, tuned to  $E_2$ .

will be needed in order to test the coupling methods over a large selection of such glasses. Furthermore, the affect of different string characteristics, such as impedance, material and gauge on the glass reaction could be explored in both experiment and simulation. Another possible direction of research is the usage of modern methods such as 3-D printing for bridge fabrication. Such methods might allow designing bridges of more elaborate geometries and from different materials.

Each of the methods described in this research may be used as the basic operating mechanism for future instruments. The design may limit the choice of glasses to a specific geometry in order to fully use the capabilities of the optimized bridge. An alternative approach might require the development of additional optimized bridges, custom fitted to various glass geometries.

In conclusion, we have explored a new method of exciting wine glass sounds: coupling to a plucked string. Two coupling methods were proposed: direct contact between a string to glass or using a custom designed coupling component. An optimized coupling component was developed using two optimization methods and was shown to increase the intensity of the generated sounds. Each coupling method provides a different approach for the design of new wine glass based instruments. It is our hope that the coupling methods developed in this research will be used as the basis for the design of future wine glass instruments, which will combine the sounds of string instruments with the rich sound spectra of wine glasses.

## **8 Acknowledgements**

We would like to thank the Technion and the program of Industrial Design at the faculty of Architecture and Town Planning for their generous support of this research. Yoav Schechner is a Landau Fellow - supported by the Taub Foundation. His work is conducted in the Ollendorff Minerva Center. Minerva is funded through the BMBF. This research did not receive any specific grant from funding agencies in the public, commercial, or not-for-profit sectors.

## References

- [1] D. A. Gallo and S. Finger, “The power of a musical instrument: Franklin, the mozarts, mesmer, and the glass armonica.,” *History of psychology*, vol. 3, no. 4, p. 326, 2000.
- [2] V. Meyer and K. J. Allen, “Benjamin franklin and the glass armonica,” *Endeavour*, vol. 12, no. 4, pp. 185–188, 1988.
- [3] A. French, “In vino veritas: A study of wineglass acoustics,” *American Journal of Physics*, vol. 51, no. 8, pp. 688–694, 1983.
- [4] G. Jundt, A. Radu, E. Fort, J. Duda, H. Vach, and N. Fletcher, “Vibrational modes of partly filled wine glasses,” *The Journal of the Acoustical Society of America*, vol. 119, no. 6, pp. 3793–3798, 2006.
- [5] K.-W. Chen, C.-K. Wang, C.-L. Lu, and Y.-Y. Chen, “Variations on a theme by a singing wineglass,” *EPL (Europhysics Letters)*, vol. 70, no. 3, p. 334, 2005.
- [6] T. D. Rossing, “Acoustics of the glass harmonica,” *The Journal of the Acoustical Society of America*, vol. 95, no. 2, pp. 1106–1111, 1994.
- [7] F. Dunn, W. Hartmann, D. Campbell, N. Fletcher, and T. Rossing, *Springer handbook of acoustics*. Springer, 2015.
- [8] J.-L. Le Carrou, F. Gautier, and R. Badeau, “Sympathetic string modes in the concert harp,” *Acta Acustica united with Acustica*, vol. 95, no. 4, pp. 744–752, 2009.
- [9] S. Weisser and M. Demoucron, “Shaping the resonance. sympathetic strings in hindustani classical instruments,” in *Proceedings of Meetings on Acoustics 163ASA*, vol. 15, p. 035006, ASA, 2012.
- [10] B. Hopkin, *Musical instrument design: Practical information for instrument making*. See Sharp Press, 1996.
- [11] D. Godlovitch, S. Trail, T. F. Tavares, and G. Tzanetakis, “Physical modeling and hybrid synthesis for the gyl african xylophone,” in *Proc. Int. Conf. Sound and Music Computing (SMC)*, 2012.

- [12] McGraw-Hill, *McGraw-Hill concise encyclopedia of physics*. McGraw-Hill Companies, 2005.
- [13] W. Rueckner, D. Goodale, D. Rosenberg, S. Steel, and D. Tavilla, “Lecture demonstration of wineglass resonances,” *American journal of physics*, vol. 61, no. 2, pp. 184–186, 1993.
- [14] B. Berner, “Resonant wineglasses and ping-pong balls,” *The Physics Teacher*, vol. 38, no. 5, pp. 269–270, 2000.
- [15] M. P. Bendsoe and O. Sigmund, *Topology optimization: theory, methods, and applications*. Springer Science & Business Media, 2013.
- [16] Y. Yu, I. G. Jang, and B. M. Kwak, “Topology optimization for a frequency response and its application to a violin bridge,” *Structural and Multidisciplinary Optimization*, vol. 48, no. 3, pp. 627–636, 2013.
- [17] M. P. Bendsoe and N. Kikuchi, “Generating optimal topologies in structural design using a homogenization method,” *Computer methods in applied mechanics and engineering*, vol. 71, no. 2, pp. 197–224, 1988.
- [18] J. Taylor, *Tone production on the classical guitar*. Musical New Services, 1978.
- [19] R. J. Ross *et al.*, “Wood handbook: wood as an engineering material,” 2010.
- [20] M. P. Bendsoe and O. Sigmund, “Material interpolation schemes in topology optimization,” *Archive of applied mechanics*, vol. 69, no. 9, pp. 635–654, 1999.
- [21] P. W. Christensen and A. Klarbring, *An introduction to structural optimization*, vol. 153. Springer Science & Business Media, 2008.
- [22] G. Bharaj, D. I. Levin, J. Tompkin, Y. Fei, H. Pfister, W. Matusik, and C. Zheng, “Computational design of metallophone contact sounds,” *ACM Transactions on Graphics (TOG)*, vol. 34, no. 6, p. 223, 2015.

- [23] D. Li, D. I. Levin, W. Matusik, and C. Zheng, “Acoustic voxels: Computational optimization of modular acoustic filters,” *ACM Transactions on Graphics (TOG)*, vol. 35, no. 4, p. 88, 2016.
- [24] G. Koopmann and A. Belegundu, “Tuning a wine glass via material tailoringan application of a method for optimal acoustic design,” *Journal of sound and vibration*, vol. 239, no. 4, pp. 665–678, 2001.
- [25] J. W. Murphy, J. McVay, A. Kapur, and D. A. Carnegie, “Designing and building expressive robotic guitars.,” in *NIME*, pp. 557–562, 2013.
- [26] T. Smit, F. Türckheim, and R. Mores, “A highly accurate plucking mechanism for acoustical measurements of stringed instruments,” *The Journal of the Acoustical Society of America*, vol. 127, no. 5, pp. EL222–EL226, 2010.